Letters in Applied NanoBioScience
Open-Access Journal (ISSN: 2284-6808)

Article
Volume 14, Issue 1, 2025, 45
https://doi.org/10.33263/LIANBS141.045

Synthesis, Characterization, and Photocatalytic Applications of ZnO-Fe_2O_3/PVA Nanocomposite

Mahesh Bhat [1,*], Ere Vijaya Sekhar [2], Belakavadi Kalaiah Sagar [3]

[1] Department of Chemistry, Poornaprajna College, Udupi 576101, Karnataka, India
[2] PG Department of Chemistry, JSS College for Women, Saraswathipuram, Mysore-570 009 Karnataka, India
[3] Department of Studies in Chemistry, University of Mysore, Mysore-570 006, Karnataka, India
* Correspondence: maheshbhat@ppc.ac.in (M.B.);

Scopus Author ID 57077906100
Received: 13.06.2022; Accepted: 7.08.2023; Published: 28.09.2024

Abstract: This present study involves synthesizing ZnO/Nanocomposite using the solution phase method. Synthesized nanocomposites have been characterized through SEM-EDX to recognize the size and shape of the synthesized nanocomposite. The particle size distribution and zeta potential of the material were determined by the DLS method. The EDX determined the elemental percentage, and the consequences were comparable with the anticipated calculations. This nanocomposite material was efficiently utilized for photocatalytic degradation of the various dyes in the aqueous solution. Batch operations were carried out in the liquid phase to examine the impact of pH on the degradation capacity of Congo red, Crystalline violet, and Methyl red nanocomposite doses, and the optimum conditions for these parameters were evaluated. The outcome indicates that the nanocomposite can be used as a good low-cost alternative for treating effluents containing organic dyes.

Keywords: ZnO; PVA; nanocomposite; SEM-EDX; photocatalyst; dyes.

1. Introduction

Nanocomposites encompass a matrix wherein fillers are included based on the properties to be improved [1,2]. The organic and inorganic materials can be used as matrices and reinforcing fillers in the preparation for nanocomposites. Depending on the matrices used, nanocomposites may be classified as polymer matrix nanocomposites, ceramic matrix nanocomposites, or metal matrix nanocomposites [3,4]. The various composite materials were synthesized with multiphase solid materials; it is a mixture of more than one component, including a continuous and discontinuous phase with at least one within the nano-scaled dimension [5,6]. Because of nano compounds' wide application and materialistic properties, many studies aim to improve the synthesis process with high yield and different morphologies.

Various methodologies are reported to synthesize ZnO NPs of different morphology using various precursor materials [6,7]. The main methods include solid-state reaction, flame spray pyrolysis, mechanochemical methods, microwave-assisted technique, sonochemical method, sol-gel route [8], solvothermal [9], and hydrothermal reactions [10,11]. The co-precipitation method is also utilized to obtain the nano-sized particles of ZnO. The uniformity in ZnO particle distribution and the low reaction temperature are two important phenomena observed in all synthetic methods [12]. However, impurities and metal ions can present within the nanostructures and should be properly removed to optimize nanoparticle formation. The various morphologies of the developed ZnO include nanowires[13], nanorods [14], nanotubes

[15], nanorings, nanoplates [16], nanoflowers [17], nanobelts, and NPs. Like other NPs, ZnO also has high surface energy and can be dispersed in most solvents and polymers [18]. The traditional method of synthesizing composite materials was obtained by polymer matrix medium, which is helpful for the effective homogeneous distribution of nanoparticles [19]. This is normally achieved by selecting appropriate mixing methods, physical or chemical, to reinforce the filler in the polymers. The method can enhance the ZnO dispersion stability and also magnify proper interfacial adhesion between ZnO and polymer. In addition, the size of the nanofillers and polymer matrix properties also influence the targeted composite performance [20]. Selecting the proper mixing method for the filler reinforcement in the polymers matrix, either physical or chemical method surface modulation can be achieved; while the physical methods involve in physical state, i.e., in solutions or melting state fillers and polymers were mixed with each other, in the chemical method, involves chemical reactions which generate chemical bonds between the two components. The different types of filler and polymer present in the composite material create the connections through static interactions like Vander Waals forces or Lewis acid-base interactions in physical mixing, whereas multi-structured and stable composites with stronger polymer-filler interactions are formed during chemical synthesis [21,22].

The chemical method of grafting polymers on the ZnO surface gives homogeneous and transparent products, which can be easily separated by centrifugation [23]. During the process of polymer incorporation, observed phase separation is negligible in composite preparation, and their decomposition temperatures are often higher than that of the native polymers; these characteristics ensure good interaction between polymer-ZnO, and the stronger the interaction, the higher the stability of the nanocomposites. Such nanocomposites find a variety of applications in adhesives, electrically and thermally conductive materials, dye attachment, and encapsulations. The photoelectrochemical activity of ZnO performance can be enhanced by constructing a hetero junction with Fe_2O_3, and it overcomes the low photoelectrochemical efficiency [24].

2. Materials and Methods

2.1. Chemicals and materials.

All reagents utilized for the work are analytical grade chemicals such as Congo red, Indigo carmine, crystalline violet, $FeCl_3$•$6H_2O$, TiO_2, Polyvinyl alcohol (PVA), NaOH, and all the chemicals procured from SD Fine Chemicals India.

2.2.1. Preparation of ZnO nanocomposite.

2.027g of $FeCl_3.6H_2O$ dissolved in 50ml of water,2.0g of ZnO(solid) added to the above solution, and 2.5g of Polyvinyl alcohol (PVA) added to the above solution stirred for 30 min. During stirring, add 3g of NaOH solution, which is already dissolved in 50 ml H_2O; continue stirring until the precipitate is obtained; the obtained precipitate is filtered and washed with water, and the residue is kept in a hot air oven at 200°C for 2hr. After drying, the obtained product was ground well until it became a fine powder. The powder was sieved so that all the particles would be a uniform size. Finally, the ZnO nanocomposite powder was stockpiled in an airtight container and utilized for further studies without further treatment.

2.2.2. Dye solution.

Aqueous solutions of varied concentrations of Congo red, Crystalline violet, and Methyl red dyes were prepared by dilution from their stock solution, and the study was done by varying different parameters like contact time, the amount of adsorbent used, the adsorbent dosage, and the initial concentration of the solution.

2.2.3. Experimental procedure.

Batch techniques were utilized to study the photocatalytic degradation of Congo red, Crystalline violet, and Methyl red dyes using ZnO nanocomposite powder. Firstly, the stock solution of 50 mg/1ltr of dye was prepared by dissolving all three dyes in water. Three dye solutions of concentration 50 ppm each were prepared from the stock solution, and 0.0025 grams of adsorbent, i.e., ZnO nanocomposite powder, was added and incubated for 1,2,3,4 and 5h. The solution with adsorbent was kept under stirring conditions for around 5 h at 300rpm under normal conditions. After 5 hours, it was taken out and centrifuged at 8000 rpm for 10 minutes to separate all the undissolved particles. Then, both the solutions, the solution with adsorbent and the one without the adsorbent, were analyzed using a UV-Vis spectrophotometer at maximum absorbance. The results obtained from the spectroscopy confirmed that a considerable amount of dye was oxidized upon adding ZnO nanocomposite powder. Thus, we further focused our study only on ZnO nanocomposite adsorbent. Prepared the different solutions with varying concentrations of 10-50 ppm.The same procedure was applied, plotting the results to get the calibration curve.

2.2.3.1. Study of contact time.

A dye solution of 0.0125g was set by diluting the stock solution. This solution was maintained at a pH of 2, and 0.25 of adsorbent was added to it. Then, the solution was kept under stirring for 2.5h at room temperature and then taken out at different intervals. Finally, all the samples of different time intervals were examined and compared with the control without adsorbent to determine the percentage removal of dye and the effect that the contact period has on it.

2.2.3.2. Effect of contact time (concentration).

The impact of contact time on photo-oxidative degradation of 3 dyes (Congo red, Crystal violet, and Methyl red). The figure depicts that the rate of oxidative degradation is very high initially. But at later stages, the rate of degradation decreases. The concentration of dye degradation remains constant after 5 h. Hence, 5 h incubation is considered the best suitable equilibrium time for photocatalytic degradation of dyes. This is mainly due to the saturation of these active sites on the nanocomposites. This can be explained by the fact that initially, the number of sites on the surface is very large, allowing oxidative degradation to occur very easily. But over time, the active sites get saturated, reducing the rate after 5 h.

2.2.3.3. Effect of pH.

The pH of the aqueous solution plays an important role in the dye degradation process. Initially, the photocatalytic degradation experiments were carried out using CR dye. The solution of CR dye with an initial concentration of 0.005g ZnO at different pH was kept in dark

at 37°C for 30 min. Further same samples were exposed to sunlight to perform photocatalysis experiments and examine degradation ability at different time intervals.

The results showed that in the reaction period of 5 h, CR dye solutions were rapidly degraded with high efficiency at all pH. Particularly at pH 2 the removal increases from 60% (by photocatalytic degradation) to about 75% removal of CR occurs within 2.5 h, then reaches 95% by increasing the time to 5 h. At pH 8, the percent removal of CR increased from 9% (removed by photocatalytic degradation) to 60% degradation in the first 150 min, then reached 98.7% after 300 min. However, the % removal of CR dye by dark photocatalytic degradation process at pH 2 was higher than at pH 8. This result can be attributed to the point of zero charges (PZC) of the surface of ZnO, which was determined by the solid addition method and found to be at pH 7.6 solution of CR dye after the photocatalytic experiment at pH(2 and 8). Hence, the charge on the surface of ZnO at pH 2 is positive; this will facilitate the photocatalytic degradation of CR as an anionic dye, while a negative of the surface at pH 8 would minimize the photocatalytic degradation of CR dye. Secondly, the high degree of photocatalytic degradation of CR at pH5 would increase the photocatalytic degradation by adsorbed OH radicals.

The disappearance of CR dye at pH 2 was mainly due to photocatalytic degradation. The solution's final color intensity is much less compared to the original color of the starting concentration of 0.005 mg/L CR dye. It can be concluded that at pH 5 the removal of CR dye is due to a competition between photocatalytic degradation and photocatalysis processes. Also, the decrease in the rate of photocatalysis at pH 2 may be due to the increase in the concentration of the adsorbed CR dye onto the surface of ZnO. Adherence of the dyes on the surface of the nanocomposite would cover the active sites and absorb the amount of sunlight, minimizing further photocatalytic degradation. At pH 8, a high rate of removal of CR dye (98.8%) was observed, mainly because of the photocatalytic degradation process. Even though stirring of the resultant degraded solution does not reappear, the original color (solution is very clear). This can be attributed to the high concentration of OH- ions at pH 8, which helps form more •OH radicals to degrade CR dye in the solution. Similar results were reported for different studies. Also, the presence of only 8.0% of CR on the surface of ZnO did not affect the excitation process of the photocatalyst.

3. Results and Discussion

3.1. Preparation of ZnO nanocomposite and characterization:

The ZnO/Fe_2O_3 nanocomposite using PVA was prepared using the co-precipitation method with confined morphology. The obtained ZnO/Fe_2O_3 nanocomposite was subjected to Scanning Electron Microscopic (SEM)analysis. High-resolution Scanned electron microscopy (HR-SEM) of synthesized nanoparticles was shown in Figure 1a, which clearly shows the larger size ZnO/Fe_2O_3 nanocomposite with flower-shaped morphology.

Figure 1 show the scanning electron microscopic image of the synthesized material. The particle size distribution (PDS) was analyzed using a dynamic light scattering (DLS) instrument. The particles of ZnO/Fe_2O_3 nanocomposite coated with PVA were found to be approximately 1200 nm (Figure S1b). Zeta potential measurement by DLS was considered one of the useful techniques for understanding the charge of the nanocomposite in the suspension. The charge of particles was examined and found to be - 0.1 mV. Nanoparticles with a zeta potential of −10 and +10 mV are considered neutral charges, whereas if greater than +30 mV

or less than −30 mV, it is strongly cationic and anionic, respectively. Hence the overall charge of the ZnO/Fe_2O_3 nanocomposite was found to be neutral, which may be attributed to the PVA coating on the nanocomposite.

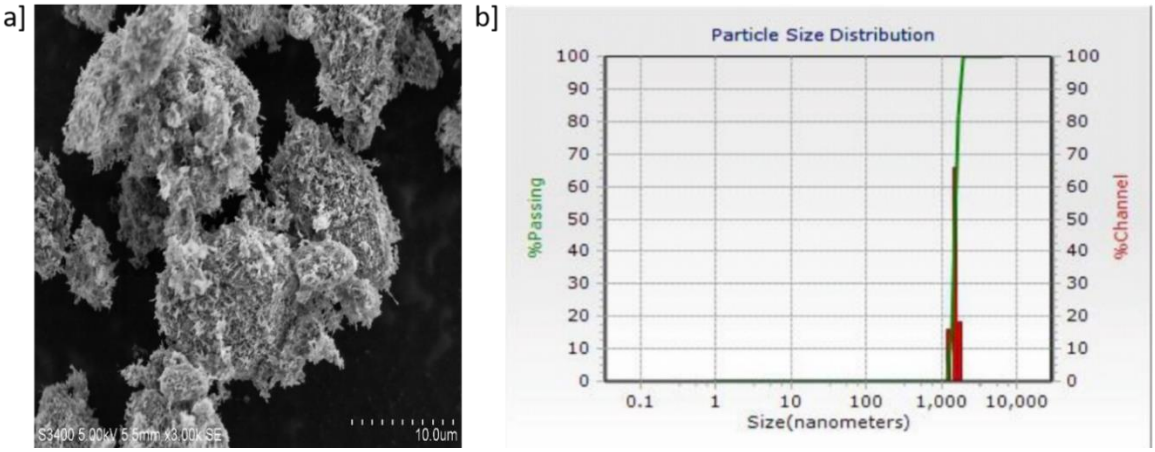

Figure 1. a) SEM images of synthesized ZnO/Fe_2O_3 nanocomposite coated with PVA. b) Particle size distribution of ZnO/Fe_2O_3 nanocomposite coated with PVA using dynamic light scattering (DLS).

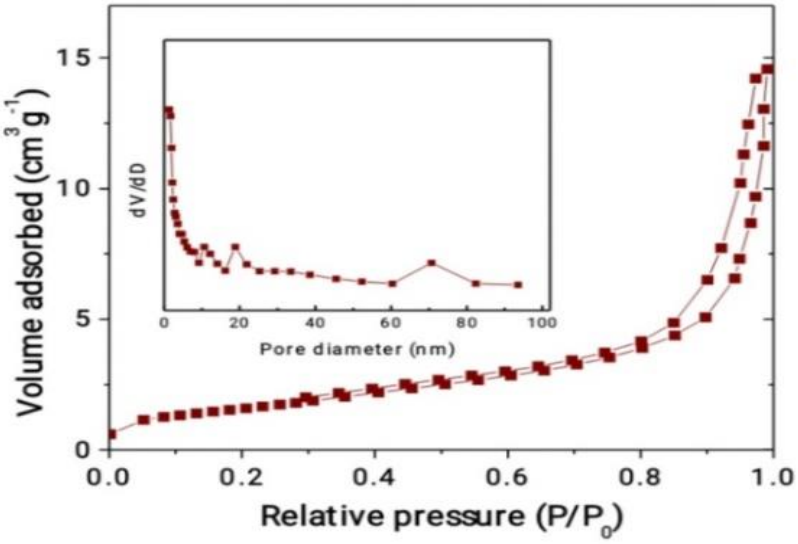

Figure 2. BET, N_2 photocatalytic degradation isotherms of ZnO/Fe_2O_3 nanocomposite.

The photocatalytic activity of nanoparticles depends upon the surface area; if the surface-to-size ratio is higher, it shows enhanced activity. The nanoparticles synthesized by the hydrothermal method resulted in the formation of nano/mesopore structures that show excellent photocatalytic performance. Photocatalysts with a high surface area are likely to absorb more dye molecules and react faster. Brunauer–Emmett–Teller (BET) surface area as a function of the pore volume of the prepared samples undoubtedly demonstrates a similar type - II curve. The BET surface area of ZnO/Fe_2O_3 was found to be 6.357 $m^2g^{-1,}$ as shown in Figure 2. As per the hysteresis loop in the relative pressure region around 0.4 - 0.9, the nitrogen photocatalytic degradation/desorption isotherms showed that the ZnO/Fe_2O_3 exhibited a similar type - IV curve. In other words, the ZnO/Fe_2O_3 existed with a mesoporous structure. The surface area of the nanocomposite repressed a huge difference in the bare nanoporous. With an increase in the surface area, a decrease in the pore size, and a large total pore volume, the nanocomposite is expected to have a high photocatalytic activity.

3.2. Photocatalytic effect of ZnO/Fe_2O_3 nanocomposite.

As prepared ZnO/Fe_2O_3 nanocomposite was used to study the photocatalytic activity against three dyes(Congo red, Crystal violet, and Methyl red). Three dye solutions were incubated with an adsorbent, i.e., ZnO nanocomposite powder, for 5 h with constant stirring under sunlight. Then it was taken out and centrifuged to separate all the undissolved particles. Then, absorbances were recorded for both test and control, and it was confirmed that a considerable amount of dye was degraded by adding ZnO/Fe2O3 nanocomposite, as shown in Figure 3. Specifically, the nanocomposite exhibits highly effective photocatalytic degradation affinity towards Congo red and Crystal violet at 87-95 %, but only 24 % degradation was observed towards Methyl red. Thus, we further focused on ZnO nanocomposite adsorbent contact time and pH effect with three dyes.

3.3. Effect on contact time with ZnO/Fe_2O_3 nanocomposite.

To test the effect of time on photocatalytic dye degradation of ZnO/Fe_2O_3 nanocomposite against three dyes analyzed. All dyes were incubated with ZnO/Fe_2O_3 nanocomposite and exposed to sunlight. The samples at different time intervals 1, 2, 3, 4, and 5h were collected and subjected to purification and UV-visible spectroscopy. The effect of contact time on the degradation of congo red is shown in Table 1, Crystal violet in Table S2, and methyl red in Table 3. This study clearly shows that ZnO/Fe_2O_3 nanocomposite shows time-dependent dye degradation. As shown in the figure the optimized time found to be 5 h for maximum dye degradation. Specifically, degradation of dye after 5 h forCongo red ~87%, Crystal violet~95%, and Methyl red~25%. However, after 5 h, dye degradation was found to be saturated. This sets the equilibrium time for photocatalytic degradation as 5 h for maximum dye degradation. This is mainly due to the saturation of the active sites in the ZnO/Fe_2O_3 nanocomposite. Hence, this study optimized the time for dye degradation.

3.4. Effect of pH on the photocatalytic affinity of ZnO/Fe_2O_3 nanocomposite.

The system's pH plays a crucial role in the photodegradation of dyes. Hence, the photodegradation of three dyes was carried out using three different pH conditions. It can be clearly seen as depicted in Figure 3 for Congo red dye, which rapidly degrades with high efficiency at neutral pH7. The dye degradation increases from 35-79% within 3 h and then reaches 87 % after 5 h. However, acid and basic and basic pH conditions were found to be less favorable. In the case of crystal violet dye degradation (Figure 4), it was found to be comparable in all pH conditions. For example, degradation after 5 h at acidic pH~95%, basic pH ~93%, and neutral pH ~87%.In the case of the last dye, Methyl red (Figure 5), the degradation by ZnO/Fe_2O_3 nanocomposite is less effective. However, among the different pH conditions, neutral seems highly efficient with ~25% degradation affinity. Hence, the ZnO/Fe_2O_3 nanocomposite has highly specific catalytic activity against neutral and anionic dyes.

Table 1. Effect of contact time on percentage of dye degradation.

CONGO RED					
Time in hour	**% of removal of dye(acid)**	**Time in hour**	**% of removal of dye(base)**	**Time in hour**	**% of removal of dye(neutral)**
1	16.2	1	7.77	1	34.58
2	19.06	2	3.86	2	75.72
3	42.86	3	5.78	3	78.52
4	47.62	4	13.48	4	79.44
5	50.30	5	19.24	5	86.92

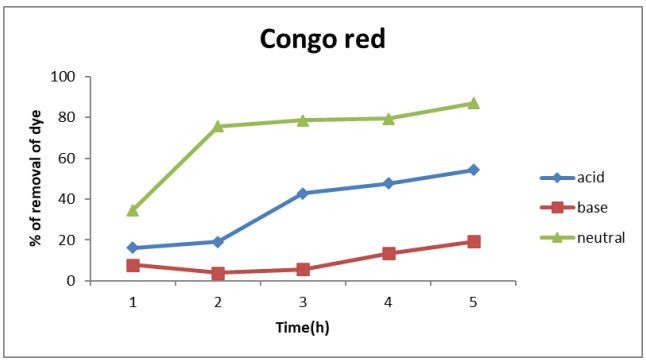

Figure 3. Effect of the pH for degradation of congo red by nanocomposite.

Table 2. Effect of contact time on percentage of dye degradation.

Crystalline violet

Time in hour	% of removal of dye(acid)	Time in hour	% of removal of dye(base)	Time in hour	% of removal of dye(neutral)
1	58.46	1	63.82	1	59.06
2	70.14	2	73.34	2	75.24
3	77.94	3	80.00	3	78.1
4	85.72	4	82.8	4	79.04
5	94.82	5	93.3	5	86.6

Table 3. Effect of contact time on percentage of dye degradation.

METHYL RED

Time in hour	% of removal of dye(acid)	Time in hour	% of removal of dye(base)	Time in hour	% of removal of dye(neutral)
1	5.92	1	8.58	1	17.76
2	8.62	2	9.15	2	17.76
3	10.76	3	11.44	3	23.08
4	11.84	4	16.58	4	23.08
5	13.98	5	20.0	5	24.2

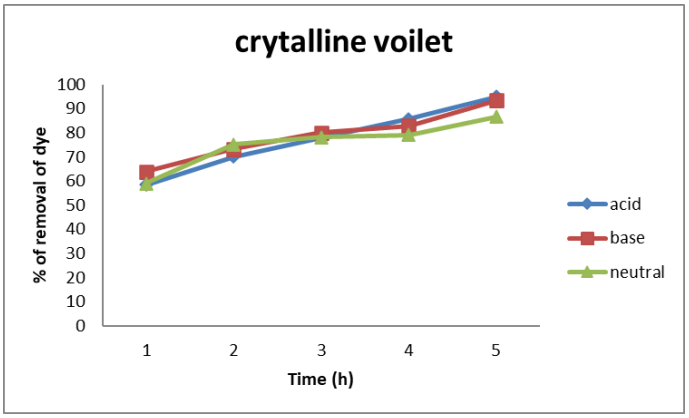

Figure 4. Effect of the pH in degradation of crystalline violet by nanocomposite.

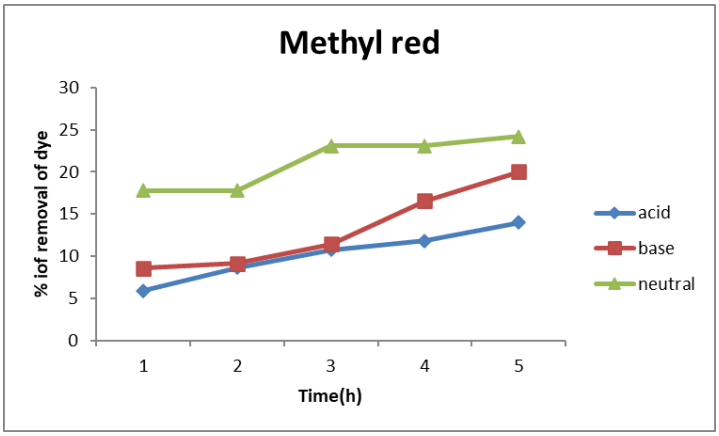

Figure 5. Effect of pH for degradation of Methyl red by nanocomposite.

4. Conclusions

In this present study, synthesized SEM characterized the ZnO nanocomposite synthesized nanomaterial for morphology characterization. SEM images show that the surface is uniform, particles are evenly distributed, and particle size is in nanometers. Further, it was analyzed by EDX for the calculation of elements and their percentage. This study depicted that synthesized material composition was up to the mark.

In the later part, the synthesized nanocomposite was evaluated for its photodegradation ability. Synthesized material was efficient in degrading the color from the aqueous phase solution. Congo red dye solution was rapidly degraded with high efficiency at ph 2. The removal increased by 60-75% within 150 min and reached 97% by increasing the time to 300 min, while the base removal of dye increased by 9% to 60% degradation in the first 150 min and then reached 98.7 % after 300 min. Then, the percentage of removal of Congo red dye by photocatalytic degradation process at acidic levels was higher than the basic pH.

Funding

This research received no external funding.

Acknowledgments

The authors gratefully acknowledge Dr. Abhishek MR for instrumentation support and Dr. Jagadeesh K for technical support.

Conflicts of Interest

The authors declare no conflict of interest.

References

1. Müller, K.; Bugnicourt, E.; Latorre, M.; Jorda, M.; Echegoyen Sanz, Y.; Lagaron, J.M.; Miesbauer, O.; Bianchin, A.; Hankin, S.; Bölz, U.; Pérez, G.; Jesdinszki, M.; Lindnner, M.; Scheuerer, Z.; Castelló, S.; Schmid, M. Review on the Processing and Properties of Polymer Nanocomposites and Nanocoatings and Their Applications in the Packaging, Automotive and Solar Energy Fields. *Nanomaterials* **2017**, *7*, 74-121, https://doi.org/10.3390/nano7040074.
2. Carey, M.; Barsoum, M.W. MXene polymer nanocomposites: a review. *Materials Today Advances* **2021**, *9*, https://doi.org/10.1016/j.mtadv.2020.100120.
3. Rathod, V.T.; Kumar, J.S.; Jain, A. Polymer and ceramic nanocomposites for aerospace applications. *Applied Nanoscience* **2017**, *7*, 519-548, https://doi.org/10.1007/s13204-017-0592-9.
4. Reduwan Billah, S.M. Composites and Nanocomposites. In: *Functional Polymers*. Jafar Mazumder, M.A.; Sheardown, H.; Al-Ahmed, A. Eds.; Springer International Publishing: Cham, **2019;** pp. 1-67.https://doi.org/10.1007/978-3-319-92067-2_15-1.
5. Sarkhel, R.; Ganguly, P.; Das, P.; Bhowal, A.; Saha, A. 14 - Industrial dye degradation bydifferent nanocomposite doped material. In: *Photocatalytic Degradation of Dyes*. Shah, M.; Dave, S.; Das, J. Eds.; Elsevier: **2021;** pp. 377-404,https://doi.org/10.1016/B978-0-12-823876-9.00011-1.
6. Nguyen, D.D. Preparation of various morphologies of ZnO nanostructure through wet chemical methods.*Advanced Materials Science***2019**, *4*, 1-5,https://doi.org/10.15761/AMS.1000147.
7. Liu, B.; Zeng, H.C. Hydrothermal Synthesis of ZnO Nanorods in the Diameter Regime of 50 nm. *Journal of the American Chemical Society* **2003**, *125*, 4430-4431,https://doi.org/10.1021/ja0299452.
8. Chen, C.; Yu, B.; Liu, P.; Liu, J.F.; Wang, L. Investigation of nano-sized ZnO particles fabricated by various synthesis routes. *Journal of Ceramic Processing Research* **2011**, *12*, 420-425.
9. Pacholski, C.; Kornowski, A.; Weller, H. Self-Assembly of ZnO: From Nanodots to Nanorods. *Angewandte Chemie International Edition* **2002**, *41*, 1188-1191,https://doi.org/10.1002/1521-3773(20020402)41:7.
10. Gu, C.; Huang, J.; Wu, Y.; Zhai, M.; Sun, Y.; Liu, J. Preparation of porous flower-like ZnO nanostructures and their gas-sensing property. *Journal of Alloys and Compounds* **2011**, *509*, 4499-4504, https://doi.org/10.1016/j.jallcom.2010.11.078.

11. Sivapunniyam, A.; Wiromrat, N.; Myint, M.T.Z.; Dutta, J. High-performance liquefied petroleum gas sensing based on nanostructures of zinc oxide and zinc stannate. *Sensors and Actuators B: Chemical* **2011**, *157*, 232-239, https://doi.org/10.1016/j.snb.2011.03.055.
12. Shaba, E.Y.; Jacob, J.O.; Tijani, J.O.; Suleiman, M.A.T. A critical review of synthesis parameters affecting the properties of zinc oxide nanoparticle and its application in wastewater treatment. *Applied Water Science* **2021**, *11*,https://doi.org/10.1007/s13201-021-01370-z.
13. Hu, H.; Huang, X.; Deng, C.; Chen, X.; Qian, Y. Hydrothermal synthesis of ZnO nanowires and nanobelts on a large scale. *Materials Chemistry and Physics* **2007**, *106*, 58-62,https://doi.org/10.1016/j.matchemphys.2007.05.016.
14. Ghannam, H.; Chahboun, A.; Turmine, M. Wettability of zinc oxide nanorod surfaces. *RSC Advances* **2019**, *9*, 38289-38297,https://doi.org/10.4172/2157-7439.S8-004.
15. Yuewen, W.; Zuolin, C. Synthesis and photoluminescence of well aligned ZnO nanotube arrays by a simple chemical solution method. *Journal of Physics: Conference Series* **2009**, *152*,1–5,https://doi.org/10.1088/1742-6596/152/1/012021.
16. Tan, S.T.; Ali Umar, A.; Salleh, M.M. (001)-Faceted hexagonal ZnO nanoplate thin film synthesis and the heterogeneous catalytic reduction of 4-nitrophenol characterization. *Journal of Alloys and Compounds* **2015**, *650*, 299-304,https://doi.org/10.1016/j.jallcom.2015.06.280.
17. Peng, S.; Wu, G.; Song, W.; Wang, Q. Application of flower-like ZnO nanorods gas sensor detecting SF6 decomposition products. *J Nanomater*.**2013**,*2013*,https://doi.org/10.1155/2013/135147.
18. Lee, W.; Yeop, J.; Heo, J.; Yoon, Y.J.; Park, S.Y.; Jeong, J.; Shin, Y.S.; Kim, J.W.; An, N.G.; Kim, D.S.; Park, J.; Kim, J.Y. High colloidal stability ZnO nanoparticles independent on solvent polarity and their application in polymer solar cells. *Scientific Reports* **2020**, *10*,https://doi.org/10.1038/s41598-020-75070-0.
19. Burlibaşa, L.; Chifiriuc, M.C.; Lungu, M.V.; Lungulescu, E.M.; Mitrea, S.; Sbarcea, G.; Popa, M.; Măruţescu, L.; Constantin, N.; Bleotu, C.; Hermenean, A. Synthesis, physico-chemical characterization, antimicrobial activity and toxicological features of AgZnO nanoparticles. *Arabian Journal of Chemistry* **2020**, *13*, 4180-4197,https://doi.org/10.1016/j.arabjc.2019.06.015.
20. Šupová, M.; Martynková, G.S.; Barabaszová, K. Effect of Nanofillers Dispersion in Polymer Matrices: A Review. *Science of Advanced Materials* **2011**, *3*, 1-25,https://doi.org/10.1166/sam.2011.1136.
21. Saraswat, V.K. 6 - ZnO nanofillers–based polymer and polymer blend nanocomposites. In: *Nanostructured Zinc Oxide*. Awasthi, K. Ed.; Elsevier: **2021**; pp. 157-186,https://doi.org/10.1016/B978-0-12-818900-9.00023-1.
22. Zhang, Y.; Niu, H.; Liyun, W.; Wang, N.; Xu, T.; Zhou, Z.; Xie, Y.; Wang, H.; He, Q.; Zhang, K.; Yao, Y. Fabrication of thermally conductive polymer composites based on hexagonal boron nitride: recent progresses and prospects. *Nano Express* **2021**, *2*, 1-21, https://doi.org/10.1088/2632-959X/ac2f09.
23. Raha, S.; Ahmaruzzaman, M. ZnO nanostructured materials and their potential applications: progress, challenges and perspectives. *Nanoscale Advances* **2022**, *4*, 1868-1925,https://doi.org/10.1039/D1NA00880C.
24. Yudyanto; Aini, P.N.; Sufian, S.; Abadi, M.T.H.; Maryam, S.; Kurniawan, R.; Mufti, N. Enhanced photoelectrochemical performance of Fe2O3/ZnO nanocomposite film. *AIP Conference Proceedings* **2020**, *2228*,https://doi.org/10.1063/5.0000879.